

Review of Flight-to-Wind-Tunnel Drag Correlation

Edwin J. Saltzman and Theodore G. Ayers
NASA Ames Research Center, Edwards, California

Nomenclature

A	= cross-sectional area
C_D	= drag coefficient, D/qS
C'_D	= $C_D - C_{D_b} - C_{D_\beta}$
C_{D_b}	= base drag coefficient, D_{base}/qS
C_{D_β}	= boattail drag coefficient
ΔC_D	= $C_D - C_{D_{M=0.9}}$
C_f	= local turbulent skin friction coefficient
C_L	= lift coefficient, L/qS
$C_{N_{wp}}$	= normal force coefficient of wing panel
C_p	= pressure coefficient, $(p_l - p)/q$
D	= drag
L	= lift
i	= length of body or fuselage
M	= Mach number, freestream unless otherwise indicated
M_D	= drag divergence Mach number, $\Delta C_D/\Delta M = 0.1$
p	= freestream static pressure
$\sqrt{\bar{p}_s'^2}$	= average root-mean-square pressure fluctuation amplitude
q	= dynamic pressure, $0.7M^2p$
R	= Reynolds number, $(U_l)/\nu$
S	= wing reference area
T	= temperature
T'	= reference temperature
t/c	= wing thickness-to-chord ratio
U	= freestream velocity
x/c	= wing-chord location
α	= angle of attack
δ_a	= aileron deflection
δ_e	= elevon deflection
Λ	= wing sweep angle
ν	= kinematic viscosity

Subscripts

e	= edge conditions
l	= local
s	= static pressure at cone surface
t	= total or stagnation value
w	= wall
x	= distance from leading edge of cylinder
0	= zero lift
∞	= freestream conditions

Superscripts

$(\bar{})$	= incompressible
$()'$	= reference temperature method (also called T' method)

Abbreviated Wind-Tunnel Names

UPWT	= Unitary Plan Wind Tunnel, NASA Langley Research Center
16 ft TT,	
16' TT	= 16 ft Transonic Tunnel, NASA Langley Research Center
8 ft TT-CAL	= 8 ft Transonic Tunnel, Calspan Corporation
8 ft TPT,	
8' TPT	= 8 ft Transonic Pressure Tunnel, NASA Langley Research Center

Introduction

MOST increments of improvement in aircraft performance have their origin in model testing, most often wind-tunnel models. This approach, which was used at times even by the Wright brothers, remains a key element in the development of configurations that are more efficient, have more endurance, or perform over a more extensive range of speed or lift.

Mr. Saltzman is employed as a performance-aerodynamics engineer for the NASA Dryden Flight Research Facility. He has been involved with the in-flight measurement, analysis, and documentation of aircraft performance and efficiency since 1958, the formation of NASA. Prior to that time he performed similar tasks, since 1951, with the High Speed Flight Station of NACA, the parent agency of NASA. Since 1972, Mr. Saltzman's interests in aircraft efficiency have also led him to perform experimental work on ground vehicles, primarily studying practical methods of reducing the drag of high volume vehicles such as trucks and motor homes. He received a B.S. in Physics from Iowa Wesleyan College in 1950.

Ted Ayers has 24 years of government service including 17 years at the NASA Langley Research Center. He has a B.S. in Aeronautical Engineering from Northrop Institute of Technology and has devoted most of his career to research in transonic aerodynamics with emphasis on the application of supercritical aerodynamics to high performance aircraft. His Langley experience also included the systems technology aspects of advanced technology transports including the integration of aerodynamics, propulsion, and controls. In 1976, Mr. Ayers transferred to the NASA Hugh L. Dryden Flight Research Center where he served as the Chief of the Aeronautics Branch with responsibility for flight research in the Aerodynamics, Propulsion, and Structures disciplines. He is presently the Deputy Director of Flight Operations for Ames Research Center, Dryden Flight Research Facility. Mr. Ayers is a Member of AIAA.

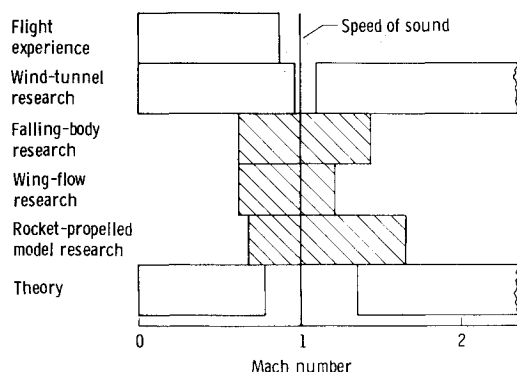


Fig. 1 The range and sources of aerodynamic knowledge as of early 1947.

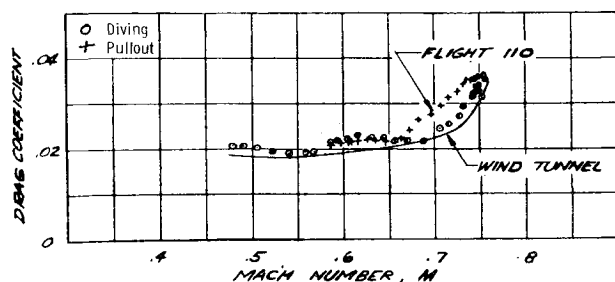
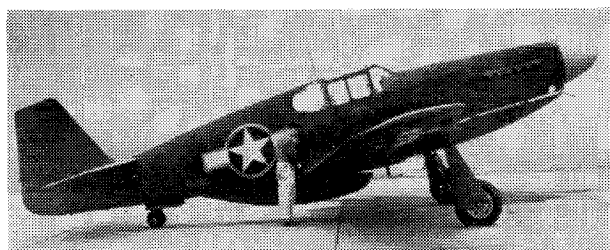


Fig. 2 Comparison of drag coefficients of the P-51B airplane as derived from flight and wind-tunnel tests.

Although aircraft designers must depend heavily upon model data and theory, their confidence in each should occasionally be bolstered by a flight demonstration to evaluate whether ground-based tools can indeed simulate real-world aerodynamic phenomena. Over the years, as the increments of improvement in performance have become smaller and aircraft development costs have risen, casual model-to-flight drag comparisons have sometimes given way to very comprehensive correlation efforts involving even more precise sensors, the careful control of variables, and great attention to detail on behalf of both the tunnel experimenters and their flight counterparts.

Examples of both the somewhat casual model-to-full-scale flight drag comparisons and the more comprehensive correlations of local aerodynamics are given in this "look-back," which reviews some of the flight-to-wind-tunnel and flight-to-flight data comparisons that have been made within the experience or the cognizance of the authors. The review reaches back to shortly after World War II, when compressibility effects became a commonly recognized barrier to further increases in aircraft speed. From that period, the review progresses forward to relatively recent flight experience.

This compilation should not be considered historical; rather, it is a somewhat narrow review of flight and wind-tunnel-model drag tests by two engineers whose concerns include the business of flight testing and flight research. It is intended for this review to provide a degree of insight into

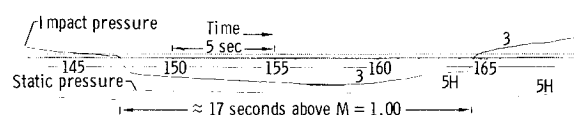
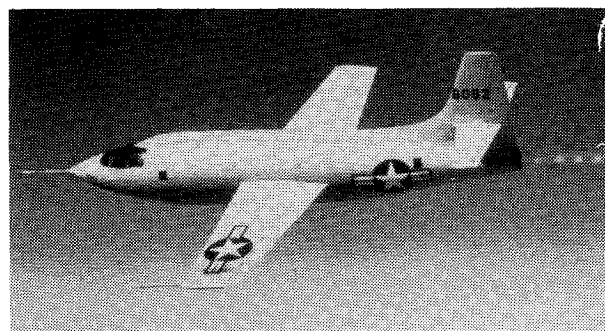


Fig. 3 XS-1 (X-1 No. 1) in powered flight and historic first recorded Mach jump, Oct. 14, 1947.

situations where model testing has been adequate and those where, conversely, the simulation of full-scale flight flow conditions has been inadequate. Methodology is not emphasized, although it is mentioned occasionally when it gives perspective. Primary emphasis is on drag components influenced by transonic conditions over the external surfaces of a variety of configurations; however, wind-tunnel and flight examples of the variation of compressible turbulent skin friction with Reynolds number are also included.

Drag Divergence Mach Number

At the beginning of World War II most bombers flew at speeds not much over 200 mph and the fighters could reach speeds of approximately 325 mph in level flight. By the end of the war some bombers could attain the fighter speeds of only 5 or 6 years earlier, the fastest propeller-driven fighters could reach 500 mph, and the earliest jet fighters were able to go about 50 mph faster. Thus, over a span of about 7 years fighter aircraft advanced from flow conditions which were predominantly incompressible to what became known as the drag divergence Mach number M_D .

During the early to mid-1940s few wind tunnels were designed for obtaining transonic data, so several ingenious methods were developed for obtaining data through the speed-of-sound region. Three such methods are represented by cross-hatched bars in Fig. 1, obtained from Ref. 1. Also shown in Fig. 1 is the gap in theory and wind-tunnel experience as of early 1947 at transonic Mach numbers and the maximum Mach number achieved in full-scale flight.

Through the falling body, wing-flow, and rocket model techniques, which are described briefly in Ref. 1, a body of transonic data developed; however, the unknown factors in transonic aerodynamics were considerably more numerous than the known. Because of the unknown Reynolds number effects for all of the experimental methods being used, and because it was uncertain how model support and tunnel wall interference effects were influenced by compressibility, it was believed that some full-scale flight data near the speed of sound would be required to evaluate the existing testing techniques, data, and theory.

An Early Experiment

An early effort to compare the onset of transonic effects on both an accurate model and a full-scale airplane was reported in Ref. 2. In this experiment the P-51B airplane was used as the test configuration. Great care was taken in both the flight and the wind-tunnel-model portions of the experiment.

The propeller (a significant modeling problem) was removed from the full-scale airplane, which was then towed to

Fig. 4 Variation of X-1 aircraft drag coefficient with Mach number for a constant lift coefficient of 0.4. a) Flight-to-flight comparison for $t/c=8$ and 10%. b) Flight-to-wind-tunnel-model comparison for $t/c=10\%$.

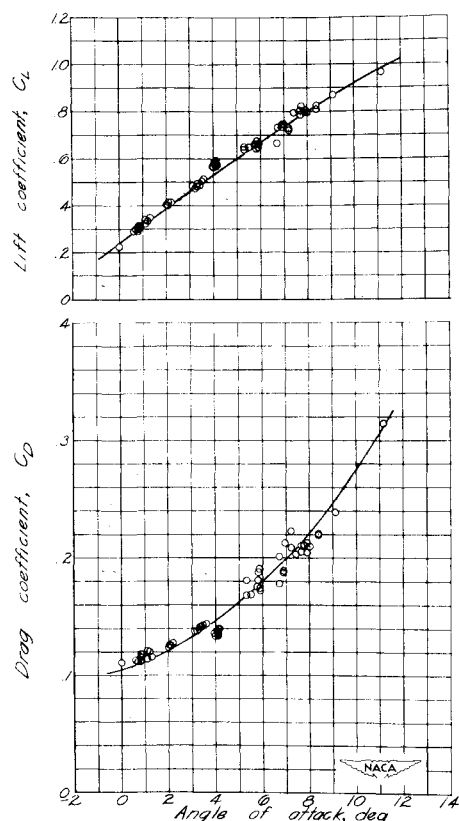
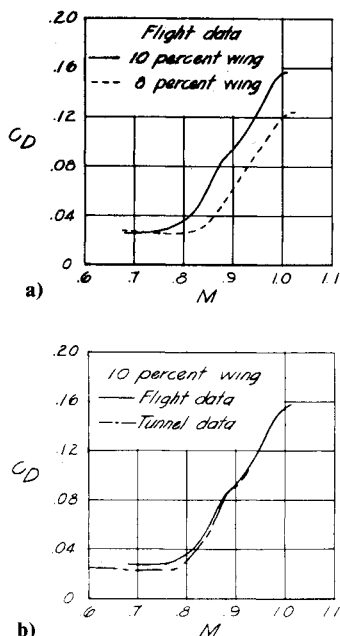


Fig. 5 The variation of C_L and C_D with angle of attack for the X-1 with the 8% thick wing ($M=1.01$).

an altitude of about 28,000 ft and released. The pilot then put the aircraft into a dive to achieve high speeds. The specially smoothed, sealed, propellerless, waxed airplane is shown in Fig. 2. The model, which was of one-third scale and constructed with great attention to detail, was tested in the then relatively new 16 ft high-speed tunnel at the NACA Ames Laboratory. The drag results from both the wind tunnel and flight are shown in Fig. 2. The authors of Ref. 2 considered the flight and model drag levels and the drag divergence Mach number to "show satisfactory agreement," thus increasing confidence in the fidelity of the flow characteristics over

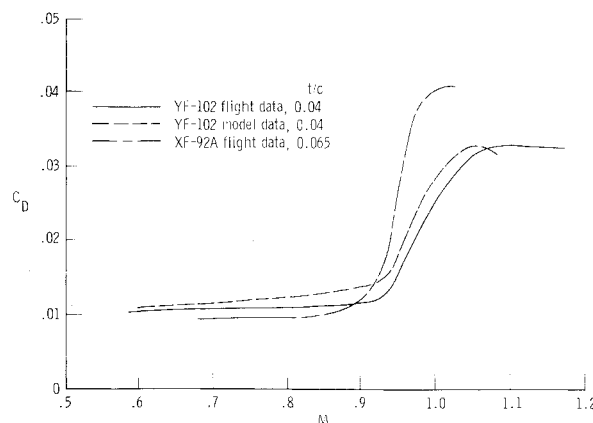
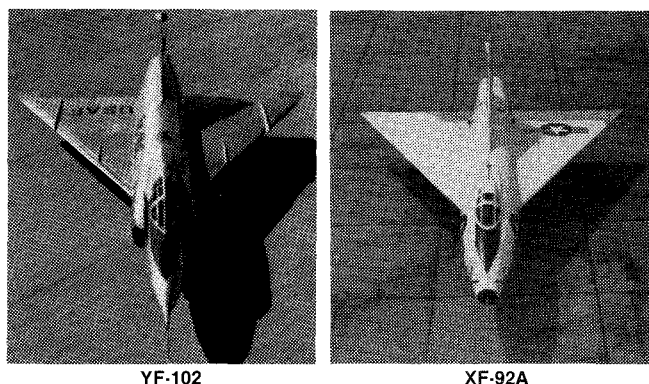


Fig. 6 Effect of wing thickness-to-chord ratio on drag divergence Mach number and the wave drag increment ($C_L=0.08$).

accurately formed models in a quality wind tunnel. The authors also noted that the flight drag coefficients were considerably larger than the wind-tunnel-model values for comparable lift coefficients during the pullout from the dive, a matter to be recalled in a table to be shown later in this review.

It is also worthy of comment that these flight lift and drag data were among the earliest obtained by the accelerometer method, thus representing a pioneering effort in obtaining what was referred to during the 1970s as dynamic performance data. During the same experiment the more traditional force method, which is related to the energy method, was also applied. In reporting the results, it was alleged that the force method produced "absurd results" because of the difficulty of accurately determining the slope of the airspeed-time curve during high-speed dives. This observation is consistent with the experience reported in Refs. 3 and 4, where these methods are compared. Thus, the accelerometer method became a trusted, easily applied technique; it has been used for even some of the most recent research aircraft.

Through the Speed of Sound with Unswept Wings

During the last two years of World War II, both the U.S. Army and the U.S. Navy became interested in designing airplanes especially to explore the Mach number region near the speed of sound. With the technical advice of the National Advisory Committee for Aeronautics (NACA), each organization financed the construction of an unswept-wing single-place monoplane. The Navy's D-558-I airplane was turbojet powered; the Army's X-1 (originally the XS-1) was rocket powered and launched from a modified B-29 bomber, which permitted the X-1 to begin powered flight at an altitude of about 25,000 ft. It was expected that from this altitude the X-1 would have sufficient total impulse to reach sonic velocity.

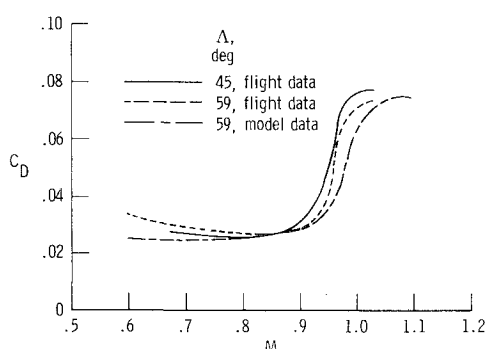
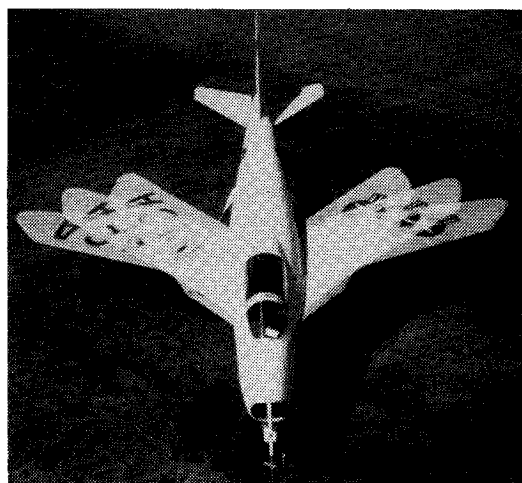


Fig. 7 Effect of wing sweep on drag divergence Mach number for X-5 airplane ($C_L = 0.2$).

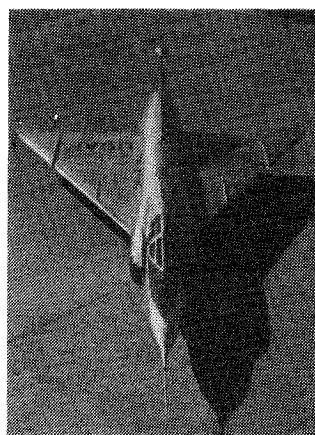
The X-1 No. 1 (Fig. 3), which had an 8% thick wing, became the first manned airplane to exceed the speed of sound. Figure 3 shows a section of the airspeed-altitude recording which documented the first in-flight Mach jump. As can be seen by the time scale, sonic velocity was seemingly exceeded for approximately 17 s. The X-1 actually exceeded the speed of sound for about 20 s, when corrections for compressibility effects are considered.

Because the companion aircraft, X-1 No. 2, had a 10% thick wing, a comparison of the transonic drag data from the two aircraft offered a chance to observe the effect of wing thickness on drag divergence Mach number in flight. As can be seen in Fig. 4a, the thicker wing caused drag divergence to occur at a Mach number about 0.06 lower than the 8% thick wing for a lift coefficient of 0.4 (also notice the difference in the transonic drag increment). At a lift coefficient of 0.2 the difference in M_D was about 0.03. Figure 4b compares the same 10% thick wing data with corresponding 1/16-scale-model results, and the drag divergence Mach numbers agree within about 0.015. These summary power-off, or coasting, flight and wind-tunnel-model data were originally reported in Refs. 5-7, and some earlier power-on flight results were reported in Ref. 8.

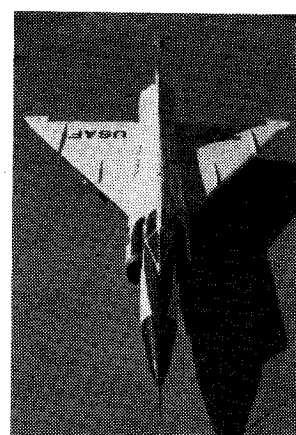
It may be of interest, while discussing the first manned airplane to exceed sonic velocity, to include the first supersonic drag polar obtained in flight. These data are shown in Fig. 5. Because no wind-tunnel-model data were available for a complete thinner winged airplane, these flight data cannot be compared with model results.

Delta Wings

New configurations were developed and flown in rapid succession during the early and mid-1950s, and for reasons of safety, the emphasis in the flight testing was on handling qualities, stability and control, and load distribution. Usually,



Prototype airplane, YF-102



Modified airplane, F-102A

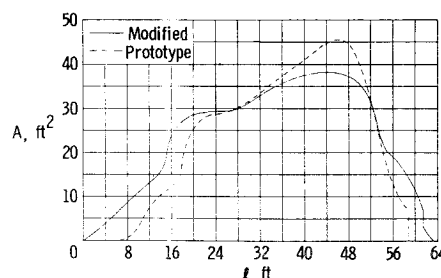


Fig. 8 Airplanes involved in full-scale transonic drag rise evaluation and the area development of each.

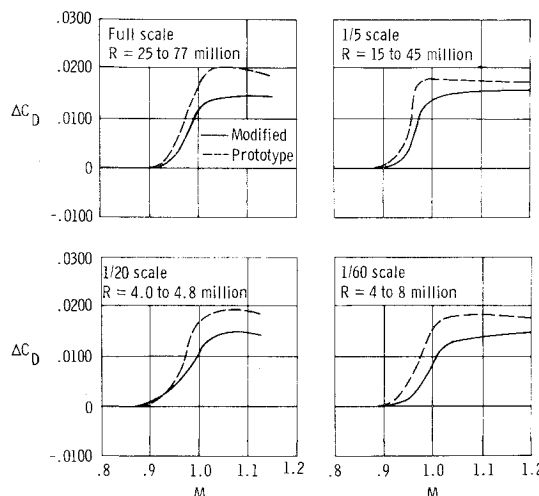


Fig. 9 Transonic drag rise characteristics of YF-102 (prototype) and F-102A (modified) full-scale configuration, 1/5-scale and 1/20-scale models, and 1/60-scale equivalent-body models.

however, the instrumentation was sufficient to permit lift and drag data to be obtained as well. Although wind-tunnel-model data were not available for every configuration, flight-to-model and flight-to-flight comparisons could be made often enough to maintain confidence in wind-tunnel-derived performance increments resulting from incremental configuration changes. An example of how periodic model and flight testing reinforced each other is shown in the XF-92A and YF-102 airplanes. Both airplanes had 60 deg delta wings and 60 deg delta tails. The former had a 6.5% thick wing⁹ and the latter a 4% thick wing.¹⁰ Figure 6 shows photographs of the airplanes and the variation, for each, of the drag coefficient with Mach number. The drag divergence Mach number is about 0.03 higher for the YF-102 configuration, which had the thinner wing, and the wave drag increment is about two-

birds of that for the thicker wing. The YF-102 model experienced drag divergence very close to the full-scale airplane but also shows evidence of transonic drag creep at speeds below drag divergence. Wind-tunnel-model results are available for only one of the configurations, that of the YF-102.

Swept Wings

The somewhat unorthodox Bell X-5 research airplane began flying in mid-1951. The wing sweep of this airplane could be varied in flight from 20 to 59 deg. The wings also translated fore and aft as wing sweep changed in order to maintain an acceptable relationship between the center of gravity and the aerodynamic center.

This rather chubby airplane clearly showed how increasing wing sweep delayed the effects of compressibility; in tests of both the full-scale aircraft in flight and of a model in a relatively sophisticated slotted-throat tunnel,¹¹⁻¹⁴ it also revealed how compressibility affected the measurement of drag at speeds immediately adjacent to that of sound. The results are shown in Fig. 7, where it is evident that the 59 deg wing sweep configuration undergoes drag divergence at a Mach number about 0.03 higher than the 45 deg wing sweep configuration, and the 59 deg wing sweep wind-tunnel and flight values of drag divergence Mach number agree. Even though the flight and model data for 59 deg of wing sweep coincide for drag divergence, there is a 12% difference in drag coefficient between the two sources of data at Mach 1.0. This illustrates the increasing difficulty of defining drag coefficient very near a Mach number of 1, both in the wind tunnel and in flight. In view of the agreement at the drag divergence Mach number, the present authors suspect that at Mach 1 the aft portions of the model fuselage did not undergo the same flow conditions as the airplane.

Transonic Drag Rise and the Area Rule

A revolutionary concept in the design of supersonic airplanes was developed during 1951 by Richard T. Whitcomb and his co-workers at the NACA Langley Aeronautical Laboratory. The discovery was based on the premise that "near the speed of sound the zero-lift drag rise of a wing-body configuration generally should be primarily dependent on the axial development of the cross-section areas normal to the airstream."¹⁵ The data supporting this principle showed that the transonic drag increment was virtually the same for a wing-body combination as for a body alone which had the same cross-sectional area development, that is, an equivalent body.

The excellent simulation of the wing-body transonic drag rise increment (wave drag) by the equivalent body analogy led rather naturally to the design principle of smoothing the area development. This was done by reducing the surface slopes of the entire aircraft (both the area growth and, past the maximum value, the area decay) through judicious lengthening, indenting, and volume addition.

A well-known application of this smoothing process, popularly known as the area rule, was the F-102A airplane. The F-102A and the prototype YF-102, which needed the smoothing, are shown in Fig. 8 in views that reveal both the fuselage indenting and the aft-located added volume. Figure 8 also shows plots of the area development for each.

Figure 9 shows the transonic drag rise increment of both aircraft as obtained in full-scale flight.¹⁶ Also shown are similar data from pairs of 1/5-scale rocket-launched models, 1/20-scale wind-tunnel models, and 1/60-scale equivalent bodies.

The data from the several sources demonstrate the effectiveness of the area smoothing process and the adequacy of the equivalent body toward the simulation of wave drag for a complete wing-body configuration.

The relatively smaller wave drag difference between the two 1/5-scale models, particularly at Mach numbers above 1.0, is

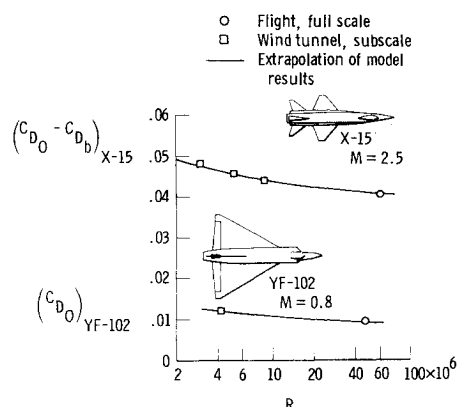


Fig. 10 Comparison of extrapolated wind-tunnel-model drag with full-scale flight results.

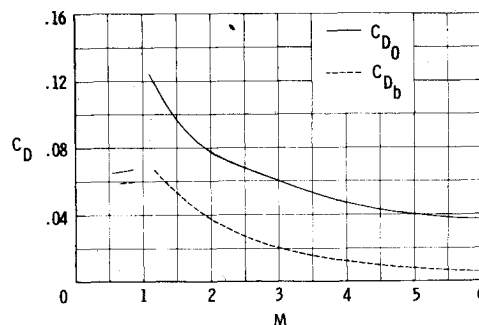
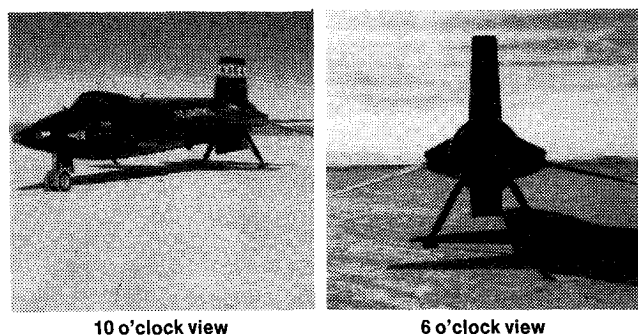


Fig. 11 Comparison of zero-lift drag and base drag for X-15 (power-off flight).

believed to be caused by relatively smaller differences in the afterbody geometry for this pair of models as compared to the other pairs.

Reynolds Number Effects

Viscous drag data obtained almost 200 years ago (actually 1796-1798) show that scale and velocity affect skin friction¹⁷; and NACA airfoil research of the 1930s and 1940s revealed the advantages of maximizing laminar flow.¹⁸ However, during the earliest years of transonic wind-tunnel and flight testing, Reynolds number effects and the friction component of drag were not given much attention for fighter configurations. This would seem to be confirmed by the fact that the wind-tunnel tests reported in Refs. 7, 13, and 15, dealing with the X-1, the X-5, and Whitcomb's early transonic drag-rise experiments, did not use or make any mention of grit or wires to fix the location of boundary-layer transition. This was probably because the transonic drag increments attributable to thickness, sweep, and aspect ratio were large in comparison to the Reynolds number effects.

Whitcomb, however, realized during his drag-rise experiments that the equivalent-body principle provided less fidelity when applying fuselage indenting than for his other applications, and he suggested that boundary-layer effects not

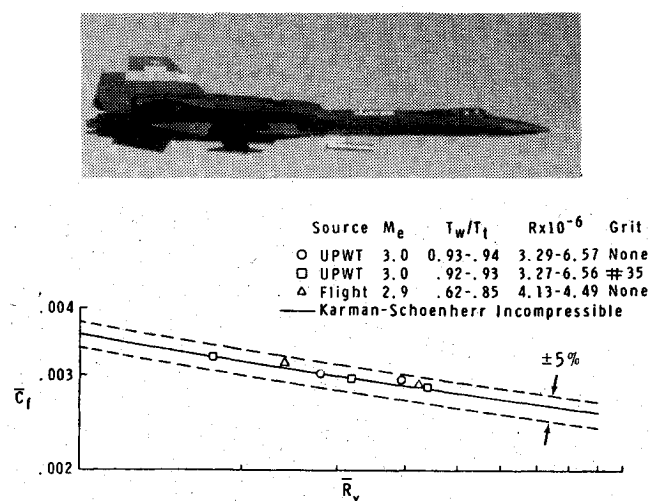
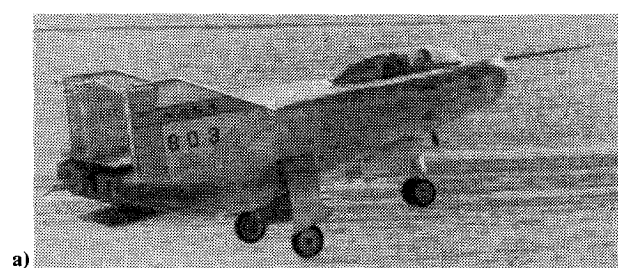


Fig. 12 Variation of local incompressible skin friction coefficient for turbulent flow with Reynolds number (T' compressibility transformation^{21,22}).



a)
 ○ Flight, full scale
 □ Model, subscale
 — Extrapolation of model results^{21,22}

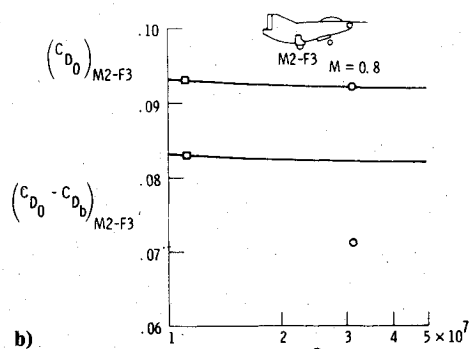


Fig. 13 M-2/F-3 lifting body: a) M-2/F-3 prior to touchdown; b) comparison of model and flight drag with and without base drag.

accounted for in designing the indentation may have been the cause.¹⁵ In any event, the soon to occur rush of wind-tunnel-model testing on the various Century-series interceptor airplanes initiated the use of boundary-layer trip devices for simulating the viscous drag of these configurations.^{19,20} Thus, viscous effects received increasing attention relative to high-speed interceptors, in that a Reynolds number extrapolation was now sometimes made to wind-tunnel-measured drag data in order to obtain a better prediction of the full-scale performance. Such extrapolations were previously routine for the slower and larger bomber and transport configurations, for which long range and endurance were of more importance than speed and agility.

Friction Drag

The first time the NACA High-Speed Flight Station related the measured full-scale drag of an airplane to model data

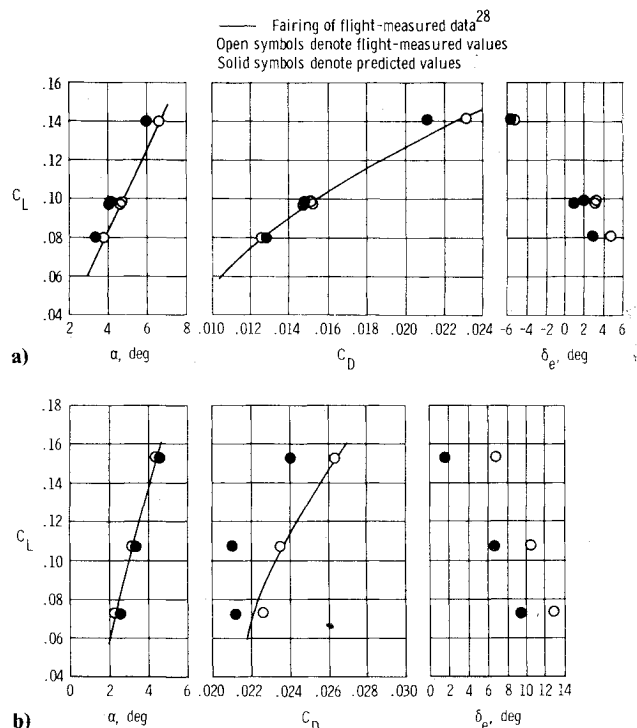
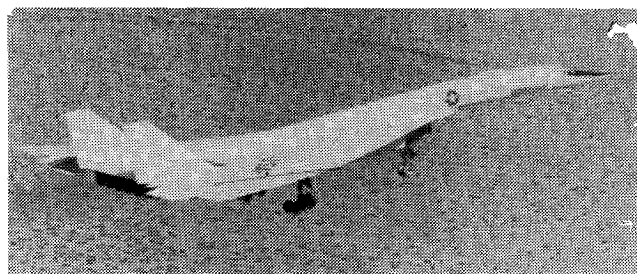


Fig. 14 Lift and drag characteristics of XB-70 airplane at supersonic cruise and transonic conditions: a) $M \approx 2.5$; b) $M \approx 1.2$.

modified by a turbulent boundary-layer extrapolation of skin friction for Reynolds number differences was during the correlation of flight and wind-tunnel data for the YF-102 airplane. This airplane was appropriate because the model had excellent geometric fidelity and had flow-through inlets and also because the basic configuration was simple (no variable inlets or complex exhaust nozzles). In addition, the full-scale airplane had aerodynamically clean surfaces, was structurally rigid, and was well instrumented for measuring thrust and drag.

The results of the correlation of the YF-102 model data and the full-scale flight data for Mach 0.8¹⁰ are shown in Fig. 10 along with the flat-plate turbulent-boundary-layer extrapolation of the model data using the Sommer and Short T' method.^{21,22}

The same methods provided a good extrapolation at supersonic speeds for the X-15 configuration (Fig. 10).^{23,24} This airplane had some of the advantages mentioned with respect to the YF-102, such as structural stiffness and simplicity of configuration, and because it was rocket powered the configuration had the added advantage of having no inlets to simulate. Furthermore, the flight data could be obtained during coasting flight, thereby avoiding the uncertainties involved in measuring thrust. The configuration's large base was a problem, however, because the model and full-scale base pressures did not agree, primarily because of wind-tunnel sting effects. Therefore, the base drag had to be subtracted from the zero-lift drag for each data source before a meaningful correlation resulted. This procedure, although it achieved the immediate goal, is not really a solution to the

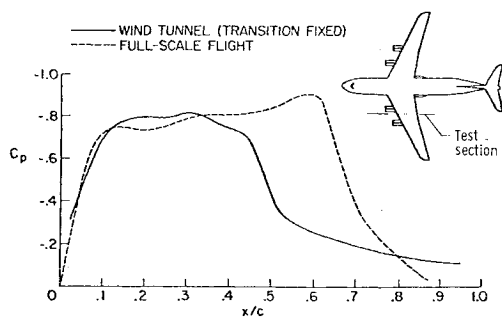


Fig. 15 Supercritical pressure distribution ($M = 0.85$).

problem of sting effects on afterbody pressure, however, and this approach to avoiding base drag discrepancies can be used only when both flight and model data are available. Figure 11 shows that a major portion of the zero-lift drag of the X-15 consisted of base drag, especially for Mach numbers below 2.

While these model and flight results for the YF-102 and X-15 configurations confirm a commonly used variation of compressible turbulent skin friction with Reynolds number, more direct flight and wind-tunnel experimental support is now available. In a unique cooperative effort between wind-tunnel and flight research teams, a hollow cylinder about 17 in. in diameter and 120 in. long was used to obtain turbulent skin friction data in both environments.^{25,26} The flight data were obtained with the cylinder mounted beneath a YF-12 airplane, and the wind-tunnel results for the cylinder were from the NASA Langley Unitary Plan Wind Tunnel. The results, shown in Fig. 12, indicate that skin friction balance data obtained in flight and from the wind tunnel are in good agreement, and both data sources confirm the Kármán-Schoenherr variation of turbulent skin friction with Reynolds number. The range of Reynolds number obtained in flight was achieved through the differences in wall temperature for the two data points.

Boattail Drag, An Occasional Modeling Problem

The aforementioned favorable correlations of the YF-102 and X-15 flight data with the extrapolated wind-tunnel-model results were made easier by the relatively small boattail angles and boattail area of these configurations. For aircraft with large boattail angles or area, or both, the preceding method of extrapolation for Reynolds number effects would probably be less successful because of the inability to simulate the location of flow separation.

The M-2/F-3 lifting body vehicle is a good example of this problem.²⁷ The configuration has a large boattail area with relatively large boattail angles (Fig. 13a). When the same extrapolation procedure that was applied to the YF-102 is applied to the M-2/F-3 (Fig. 13b, top), the wind-tunnel drag level appears to agree with the flight drag level after the wind-tunnel drag is adjusted to the flight Reynolds number. However, the wind-tunnel-model base drag values did not simulate the flight base drag values and the M-2/F-3 base area is quite large. Therefore, if the comparison is made with the base drag subtracted (lower portion of Fig. 13b), as was done with the X-15, there occurs a disagreement of approximately 15% between the extrapolated drag level and the flight results. The fortuitous circumstance wherein base drag and boattail drag differences cancelled each other is believed to be due to the difference in the location of flow separation on the full-scale and model boattail areas.

In the case of the M-2/F-3 configuration, the model boundary layer would be expected to be disproportionately thick because of the lower model Reynolds numbers. Separation would, therefore, occur at a different location over the boattail region than on the full-scale vehicle. In addition, model support and wall reflection effects are likely to modify the pressure over the base and the aft sloping surfaces.

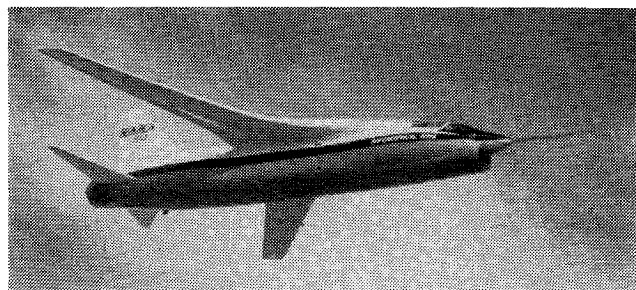


Fig. 16 Variation of drag coefficient with Mach number at design lift coefficient of 0.4.

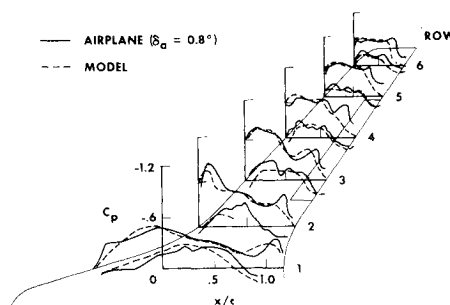


Fig. 17 Wing pressure distribution for design conditions for F-8 supercritical wing configuration ($M = 0.99$, $C_{N_{wp}} = 0.35$).

Wall Interference and Reynolds Number Effects

Large Flexible Supersonic Configuration

The large delta-winged XB-70 airplane underwent extensive flight testing during the late 1960s with very comprehensive instrumentation on board for measuring thrust and drag.²⁸ After the flight tests a rigid 0.03-scale model of the airplane was made to be representative of the steady-state flexible aircraft at Mach 2.53. The wind-tunnel model was tested at 14 Mach number/lift combinations corresponding to conditions which were recorded during steady-state flight tests.²⁹ Another part of this joint effort between NASA Centers was provided by a team from the Langley Research Center, which extrapolated the wind-tunnel-model results of Ref. 29 to the previously flown full-scale flight conditions. Predictions were made of surface deflection effects, inlet spillage, the effects of the boundary-layer trips, Reynolds number effects on skin friction, propulsion system effects, roughness, leakage, interference, and flexibility; as a result, the model base drag was subtracted in favor of flight-measured values. This procedure is reported in Ref. 30 and the resulting correlation with the flight data in Ref. 31.

Comparisons from Ref. 31 are shown in Fig. 14 for the Mach number for which the model was shaped (Mach 2.53) and for Mach 1.18. The model results for the higher Mach number are within 5% of the flight drag coefficients for the 1

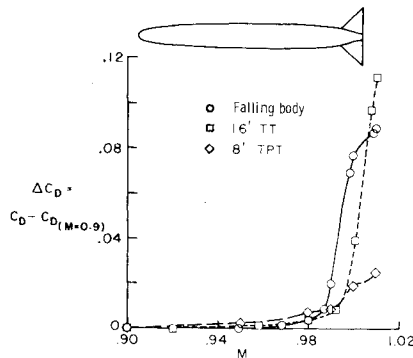


Fig. 18 Effect of wind-tunnel wall on body drag rise.

g conditions ($C_L \approx 0.1$) despite the fact that the prediction of elevon trim was about 2 deg off and that the angle of attack required to generate a specific lift coefficient was underpredicted. For Mach 1.18 the model-extrapolated drag is lower than the full-scale flight drag on the order of 10%. Corresponding model data at Mach 1.06 (not included here) were about 27% lower than the flight drag coefficients. These discrepancies for Mach numbers of 1.18 and 1.06 may represent wall interference effects on apparent required trim deflections. However, when extrapolated model drag values were adjusted to account for flight-measured trim values, about one-third of the drag discrepancy remained for level flight lift conditions. The uncertain effects of flexibility may be a significant part of the remaining drag discrepancy.

Shock/Boundary-Layer Interaction as a Modeling Problem

The mid-1960s saw a renewed interest in the transonic regime. The introduction of the modern jet airliner and visions of efficient supersonic flight generated considerable research at transonic Mach numbers. It was also during this time that unanticipated problems were encountered which adversely affected performance. One of the better known examples was the large discrepancy observed in the wing shock-wave location (Fig. 15) between the wind-tunnel and flight data obtained for the Lockheed C-141 transport aircraft at transonic Mach numbers.³² The possible effect of this discrepancy on the satisfactory prediction of loads, stability, and performance of aircraft of this type provided the impetus for new studies to resolve the differences.

The results from Ref. 32 and the new studies indicated that the disproportionate boundary-layer thickness at the model

wing trailing edge was the parameter primarily responsible for determining the shock-wave location and the resulting pressure distribution. Additional research by Blackwell³³ led to the establishment of a boundary-layer scaling criterion for airfoils with different pressure distributions. This criterion was used extensively in the development by Whitcomb and his associates at Langley of the NASA supercritical airfoil and its subsequent application to aircraft wings.

The Supercritical Wing

The relative boundary-layer thickness criterion described in Ref. 33 was indeed an important tool in providing an adequate simulation on the subscale model of the location and strength of the aft shock on the wing upper surface. The simulation was sufficient to provide a reliable prediction of the drag divergence Mach number at the design lift coefficient. As shown in Fig. 16,³⁴ the drag rise occurred a little less than 0.01 lower in Mach number in flight than for the model in the Langley 8 ft Wind Tunnel after base and boattail drag for each were subtracted. Considering how close the drag rise is to Mach 1, i.e., near 0.96, the simulation is considered to be rather good; however, the size of the model for the wind tunnel was enough to cause discrepancies which, as would be expected, grew larger as Mach 1 was approached.

An example of this may be seen in Fig. 17, where the pressure distribution for the wing panel is shown for both the model and the airplane in flight.³⁵ Figure 17 shows that the upper surface second-velocity peaks are greater in magnitude and occur farther aft in flight than on the model. In Ref. 35 Whitcomb states that the discrepancy occurs because the model airfoil shape was tuned in an environment affected by the wind-tunnel wall. This occurred as the test conditions were pushed closer to sonic velocity in spite of the model-to-test section blockage ratios being near the generally accepted value of 0.005 (it was actually 0.0056).

Data Comparisons in Retrospect

Restatement of the Data Comparisons

A review of the data we have considered shows a number of conditions that can lead to disappointing model-to-flight comparisons. A list of what we have seen appears in Table 1. The main sources of these discrepancies, all of which occur at transonic speeds, have to do with the following:

- 1) Sting-support interference effects.
- 2) Disproportionate boundary-layer (Reynolds number) effects.
- 3) Wall interference effects.

Table 1 Summary of wind-tunnel model/flight discrepancies

Aircraft	Decade	Discrepancy	Apparent cause	Remarks
P-51	Mid-1940s	Flight drag after pullout higher than for model	Different separation locations	Believe related to discussions of C-141 and M-2/F-3
X-5	Early 1950s	Drag difference at Mach 1, though the same at drag divergence Mach number	Chubby body, different separation locations	Probably differing afterbody flow
M-2/F-3	1960s	Base drag and boattail drag	Sting and different separation location	Compensating effects; fortuitous
X-15	1960s	Base drag	Sting-affected base pressure	Eliminated variable by subtracting out
XB-70	Late 1960s	Model drag too low at Mach 1.18 ^a	Tunnel wall effects	Flexibility effects may also have contributed
F-8 supercritical wing	Early 1970s	Second-velocity peak larger and farther aft in flight	Tunnel wall effects	Model too large, too close to Mach 1

^a The discrepancy in the model drag data at Mach 1.18 (and 1.06) is acknowledged to represent an off-design condition; it is presented here, however, as an example of the magnitude of a transonic discrepancy in spite of a relatively modest model-tunnel blockage ratio of 0.002.

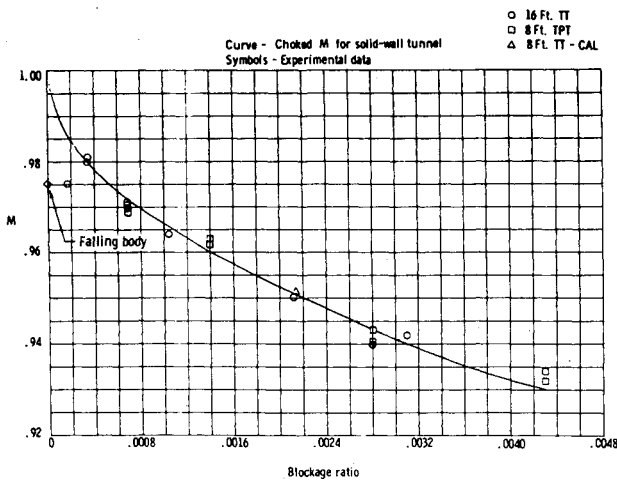


Fig. 19 Variation of transonic-creep Mach number with blockage ratio.

Sting Support Effects

Sting support effects are not great obstacles for many configurations and, where these effects are important, alternate means of support may sometimes alleviate the problem. There are also special cases when the sting support effect can at least be isolated by subtracting the base drag as was done for the X-15 or applying flight values to the model data as for the XB-70, although admittedly this can be done only for cases where the flight base pressure values are already known.

Reynolds Number Effects

The disproportionately thick model boundary layer can in some cases be accommodated through the approach discussed in Ref. 33 and as applied by Whitcomb during the F-8 supercritical wing model research. Whitcomb acknowledged that wall interference effects were an added factor that partially invalidated his efforts to deal with the disproportionate boundary layer. More will be mentioned about this matter in a following section.

From the standpoint of the wind-tunnel researcher, perhaps the most promising solution to the disproportionate boundary-layer problem is offered by the various cryogenic facilities which will soon be operational. One of these, the National Transonic Facility (NTF)³⁶⁻³⁸ will for some cases provide chord Reynolds numbers of 120 million, and it has the potential to test aeroelastic and Reynolds number effects separately by varying one factor while holding the other constant. The NTF should go a long way toward alleviating model-to-flight discrepancies such as those discussed herein.

Wall Interference Effects

The problem of wall interference effects which Whitcomb encountered encouraged him to initiate a new research effort to better understand the problem at Mach numbers very close to 1. A major part of this research involved the testing of various supercritical bodies of revolution, differing only in size, in the Langley 8 ft Transonic Pressure Tunnel and 16 ft Transonic Tunnel to assess blockage effects. Finally, carefully controlled interference-free data, for comparison with the wind-tunnel data, were obtained by using a variation of the old falling-body technique of the 1950s. The results of this research are reported in Refs. 39 and 40. A summary of the incremental drag data reported in Ref. 39 for the configuration used in the falling-body and wind-tunnel tests (Fig. 18) demonstrates the interference effects of wind-tunnel walls. While wind-tunnel wall interference was not a new discovery, the results of Refs. 39 and 40 were significant in providing quantification of such effects. Whereas a value of blockage

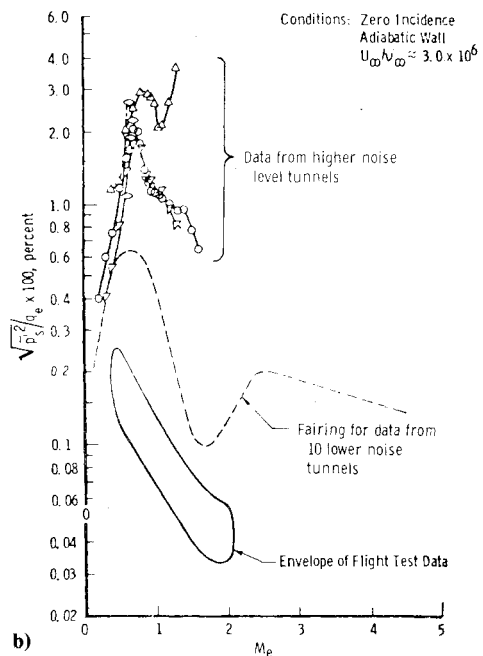
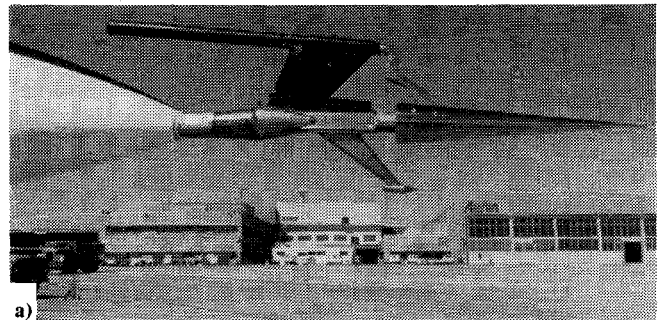
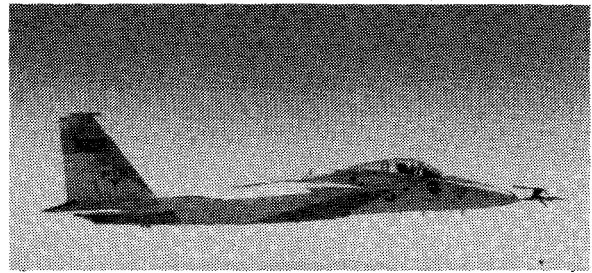


Fig. 20 Summary of results from 10 deg cone experiment: a) F-15 airplane and 10 deg cone; b) comparison of disturbance levels measured in wind tunnels with disturbances in flight.

ratio of 0.0050 was generally accepted as sufficiently low to avoid significant wall interference effects, Fig. 19 shows this not to be the case. This finding is, of course, consistent with the previously shown results from the F-8 supercritical wing wind-tunnel-to-flight comparison of chordwise wing pressure distribution. Figure 19, which shows transonic creep Mach number as a function of blockage ratio, provides experimental evidence that transonic creep Mach number may be the earliest indication of wind-tunnel wall interference near Mach 1.0.

Another promising approach to reducing wall effects is the "adaptive wall concept" wherein the most refined wind-tunnel equipment and techniques are interfaced with an on-line computer. Together they achieve a variable porosity wall capability which will tend toward a "self-correcting" facility with regard to wall effects. The concept is described in further detail in Ref. 41 and in some of its reference literature.

Alternatives for the Flight Researcher

We have mentioned some of the special efforts that the wind-tunnel researchers have made to solve some of the modeling and flow simulation problems discussed herein. Their counterparts in flight research have also had to use special means on certain kinds of tasks.

One of the most effective devices has been the local aerodynamics approach, where the aerodynamic phenomena for a single component are defined, in contrast to defining the performance of an entire airplane.

The definition of the base drag of the X-15, the wing pressure distribution for the F-8 supercritical wing, and the skin friction data from the YF-12 hollow cylinder, which have been discussed, are examples of this approach. Another such local aerodynamics experiment, which involved both flight and wind-tunnel researchers, is described in the following section.

Flow Quality and the 10 deg Cone Experiment

Although the effect of blockage can be alleviated through careful attention to model size, and the NTF and other cryogenic tunnels can reduce model size while achieving relatively high chord Reynolds numbers, there still remains the problem of wind-tunnel-induced noise. A unique wind-tunnel-to-flight correlation effort addressing this problem has been conducted by the NASA Dryden Flight Research Center and the U.S. Air Force Arnold Engineering Development Center.

A precision 10 deg cone was first used as a test configuration in 23 wind tunnels (including those in three European countries). The same cone was then flown on an F-15 airplane (Fig. 20a) at Dryden over a range of Mach number and altitude conditions. Figure 20b⁴² shows that the disturbance levels measured in all of the ground facilities, even in the lowest noise level tunnels, are significantly higher than the noise levels measured in flight. The same cone will probably be used to evaluate the flow quality of the NTF when it becomes operational.

One Last Look Back

Despite the number of aircraft and the variety of configurations discussed herein, this review is quite narrow. Transonic conditions have received most of the attention; subsonic cruise has been omitted. In addition, any comparison of the model and flight inlet and exhaust nozzle components of drag, which is discussed in several excellent works, including Refs. 43-46, had to be omitted. It may be appropriate to compile an analogous review of the propulsion/airframe components of drag after propulsion-related drag can be tested in the NTF.

At this juncture it is probably appropriate to again study Fig. 1, that is, to review the range and sources of aerodynamic knowledge as of early 1947 and to consider how differently one would draw such a figure today. We can all agree that the horizontal bar representing flight experience should now extend far to the right to Space Shuttle entry speeds⁴⁷ and that wind-tunnel research and theory also now extend to corresponding speeds. Within the transonic Mach number range considered in Fig. 1, however, and considering the problems discussed thus far in this paper, it is questionable whether the horizontal bars for the wind tunnels and theory can legitimately be changed more than slightly relative to the reliable prediction of full-scale flight drag. This is the case even for configurations that are rather ordinary, that is, for configurations not complicated by major aeroelastic deformation effects or complex airframe/propulsion system interactions. Perhaps it is true even in aerodynamics that the more things appear to change, the more they stay the same.

Concluding Remarks

Comparisons have been made of wind-tunnel-model and flight drag data for a variety of configurations representing post-World War II aircraft and airplanes of the 1960s and 1970s.

The comparisons indicate that the discrepancies between the model and flight data have much in common over the time period considered and that they primarily involve the problems caused by disproportionate boundary layers on the models (Reynolds number effects) and wall interference or blockage effects. Less prominent were sting support effects and, in the case of a large flexible airplane, the inability of the model to simulate the surface deflections for longitudinal trim.

In two instances where relatively simple, rigid, clean configurations were involved, the model-to-flight drag data confirmed the Sommer and Short T' method of extrapolating model compressible turbulent friction drag for Reynolds number effects. A unique wind-tunnel-to-flight correlation of turbulent friction drag that used the same hollow cylinder in each test also confirmed the incompressible Kármán-Schoenherr variation of turbulent skin friction with Reynolds number and the T' method for accounting for compressibility effects.

The major discrepancies discussed (Reynolds number effects, wall interference, and aeroelastic problems) will probably be less formidable when model testing is done in the new cryogenic tunnels. However, the 10 deg cone research sponsored by the U.S. Air Force and tested in flight by NASA indicates that those model tests affected by tunnel noise may, in some cases, require the lower disturbance level environment available in flight.

Some of the most decisive and useful tunnel-to-flight correlations have resulted from the local aerodynamics experimental approach wherein the aerodynamic characteristics of a single component are defined, in contrast to evaluating the performance of an entire airplane.

References

- ¹Gray, G.W., *Frontiers of Flight, The Story of NACA Research*, Alfred A. Knopf, Inc., New York, 1948.
- ²Nissen, J.M., Gadeberg, B.L., and Hamilton, W.T., "Correlation of the Drag Characteristics of a Typical Pursuit Airplane Obtained from High-Speed Wind-Tunnel and Flight Tests," NACA Rept. 916, 1948.
- ³Gasich, W.E. and Clousing, L.A., "Flight Investigation of the Variation of Drag Coefficient with Mach Number for the Bell P-39N-1 Airplane," NACA ACR No. 5D04, 1945.
- ⁴Keller, T.L. and Keuper, R.F., "Comparison of the Energy Method with the Accelerometer Method of Computing Drag Coefficients from Flight Data," NACA CB No. 5H31, 1945.
- ⁵Carmen, L.R. and Carden, J.R., "Lift and Drag Coefficients for the Bell X-1 Airplane (8-Percent-Thick Wing) in Power-Off Transonic Flight," NACA RM L51E08, 1951.
- ⁶Saltzman, E.J., "Flight Measurements of Lift and Drag for the Bell X-1 Research Airplane Having a 10-Percent-Thick Wing," NACA RM L53F08, 1953.
- ⁷Mattson, A. T. and Loving, D.L., "Force, Static Longitudinal Stability, and Control Characteristics of a 1/16-Scale Model of the Bell XS-1 Transonic Research Airplane at High Mach Numbers," NACA RM L8A12, 1948.
- ⁸Gardner, J.J., "Drag Measurements in Flight on the 10-Percent-Thick and 8-Percent-Thick Wing X-1 Airplanes," NACA RM L8K05, 1948.
- ⁹Bellman, D.R. and Sisk, T.R., "Preliminary Drag Measurements of the Consolidated Vultee XF-92A Delta-Wing Airplane in Flight Tests to a Mach Number of 1.01," NACA RM L53J23, 1954.
- ¹⁰Saltzman, E.J., Bellman, D.R., and Musialowski, N.T., "Flight Determined Transonic Lift and Drag Characteristics of the YF-102 Airplane with Two Wing Configurations," NACA RM H56E08, 1956.
- ¹¹Nugent, J., "Lift and Drag of the Bell X-5 Research Airplane in the 45° Sweptback Configuration at Transonic Speeds," NACA RM H56E02, 1956.

- ¹²Bellman, D.R., "Lift and Drag Characteristics of the Bell X-5 Research Airplane at 59° Sweepback for Mach Numbers from 0.60 to 1.03," NACA RM L53A09c, 1953.
- ¹³Bielat, R.P. and Campbell, G. S., "A Transonic Wind-Tunnel Investigation of the Longitudinal Stability and Control Characteristics of a 0.09-Scale Model of the Bell X-5 Research Airplane and Comparison with Flight," NACA RM L53H18, 1953.
- ¹⁴Bellman, D.R., "A Summary of Flight-Determined Transonic Lift and Drag Characteristics of Several Research Airplane Configurations," NASA MEMO 3-3-59H, 1959.
- ¹⁵Whitcomb, R.T., "A Study of Zero-Lift Drag-Rise Characteristics of Wing-Body Combinations Near the Speed of Sound," NACA Rept. 1273, 1957 (supersedes NACA RM L52H08).
- ¹⁶Saltzman, E.J. and Asher, W.P., "Transonic Flight Evaluation of the Effects of Fuselage Extension and Indentation on the Drag of a 60° Delta-Wing Interceptor Airplane," NACA RM H57E29, 1957.
- ¹⁷Beaufoy, M., "Recommended Definition of Turbulent Friction in Incompressible Fluids," *Nautical and Hydraulic Experiments, with Numerous Scientific Miscellanies*, Henry Beaufoy Press, London, 1834 (primary source: Locke, F.W.S., Jr., Navy Dept., Bur. of Aeronautics, Res. Div., DR Rept. 1415, June 1952).
- ¹⁸Abbott, I.H., von Doenhoff, A.E., and Stivers, L.S. Jr., "Summary of Airfoil Data," NACA Rept. 24, 1945.
- ¹⁹Osborne, R.S. and Wornom, D.E., "Aerodynamic Characteristics Including Effects of Wing Fixes of a 1/20-Scale Model of the Convair F-102 Airplane at Transonic Speeds," NACA RM SL54C23, 1954.
- ²⁰Osborne, R.S. and Templemeyer, K.E., "Longitudinal Control Characteristics of a 1/20-Scale Model of the Convair F-102 Airplane at Transonic Speeds," NACA RM SL54G15, 1954.
- ²¹Sommer, S.C. and Short, B.J., "Free-Flight Measurements of Turbulent-Boundary-Layer Skin Friction in the Presence of Severe Aerodynamic Heating at Mach Numbers from 2.8 to 7.0," NACA TN 3391, 1955.
- ²²Peterson, J.B. Jr., "A Comparison of Experimental and Theoretical Results for the Compressible Turbulent-Boundary-Layer Skin Friction with Zero Pressure Gradient," NASA TN-1795, 1963.
- ²³Hopkins, E.J., Fetterman, D.E. Jr., and Saltzman, E.J., "Comparison of Full-Scale Lift and Drag Characteristics of the X-15 Airplane with Wind-Tunnel Results and Theory," NASA TM X-713, 1962.
- ²⁴Saltzman, E.J. and Garringer, D.J., "Summary of Full-Scale Lift and Drag Characteristics of the X-15 Airplane," NASA TN D-3343, 1966.
- ²⁵Quinn, R.D. and Gong, L., "In-Flight Boundary-Layer Measurements on a Hollow Cylinder at a Mach Number of 3.0," NASA TP-1764, 1980.
- ²⁶Stallings, R.L. Jr. and Lamb, M., "Wind-Tunnel Measurements and Comparison with Flight of the Boundary Layer and Heat Transfer on a Hollow Cylinder at Mach 3," NASA TP-1789, 1980.
- ²⁷Pyle, J.S. and Saltzman, E.J., "Review of Drag Measurements from Flight Tests of Manned Aircraft with Comparisons to Wind-Tunnel Predictions," *Aerodynamic Drag*, AGARD CP-124, Oct. 1973, pp. 25-1—25-12.
- ²⁸Arnaiz, H.H., "Flight-Measured Lift and Drag Characteristics of a Large, Flexible, High Supersonic Cruise Airplane," NASA TM X-3532, 1977.
- ²⁹Daugherty, J.C., "Wind-Tunnel/Flight Correlation Study of Aerodynamic Characteristics of a Large Flexible Supersonic Cruise Airplane (XB-70-1), I: Wind-Tunnel Tests of a 0.03-Scale Model at Mach Numbers from 0.6 to 2.53," NASA TP-1514, 1980.
- ³⁰Peterson, J.B. Jr., Mann, M.J., Sorrells, R.B. III, Sawyer, W.C., and Fuller, D.E., "Wind-Tunnel/Flight Correlation Study of Aerodynamic Characteristics of a Large Flexible Supersonic Cruise Airplane (XB-70-1), II: Extrapolation of Wind-Tunnel Data to Full-Scale Conditions," NASA TP-1515, 1980.
- ³¹Arnaiz, H.H., Peterson, J.B. Jr., and Daugherty, J.C., "Wind-Tunnel/Flight Correlation Study of Aerodynamic Characteristics of a Large Flexible Supersonic Cruise Airplane (XB-70-1), III: A Comparison between Characteristics Predicted from Wind-Tunnel Measurements and Those Measured in Flight," NASA TP-1516, 1980.
- ³²Loving, D.L., "Wind-Tunnel—Flight Correlation of Shock-Induced Separated Flow," NASA TN D-3580, 1966.
- ³³Blackwell, J.A. Jr., "Preliminary Study of Effects of Reynolds Number and Boundary-Layer Transition Location on Shock-Induced Separation," NASA TN D-5003, 1969.
- ³⁴Pyle, J.S. and Steers, L.L., "Flight-Determined Lift and Drag Characteristics of an F-8 Airplane Modified with a Supercritical Wing with Comparisons to Wind-Tunnel Results," NASA TM X-3250, 1975.
- ³⁵"Supercritical Wing Technology—A Progress Report on Flight Evaluations," NASA SP-301, 1972.
- ³⁶Kilgore, R.A., Goodyer, M.J., Adcock, J.B., and Davenport, E.E., "The Cryogenic Wind-Tunnel Concept for High Reynolds Number Testing," NASA TN D-7762, 1974.
- ³⁷Kilgore, R.A., Igoe, W.B., Adcock, J.B., Hall, R.M., and Johnson, C.B., "Full-Scale Aircraft Simulation with Cryogenic Tunnels and Status of the National Transonic Facility," NASA TM-80085, 1979.
- ³⁸Adcock, J., "Simulation of Flat-Plate Turbulent Boundary Layers in Cryogenic Tunnels," *Journal of Aircraft*, Vol. 17, April 1980, pp. 284-285.
- ³⁹Usry, J.W. and Wallace, J.W., "Drag of a Supercritical Body of Revolution in Free Flight at Transonic Speeds and Comparison with Wind-Tunnel Data," NASA TN D-6580, 1971.
- ⁴⁰Couch, L.M. and Brooks, C.W. Jr., "Effect of Blockage Ratio on Drag and Pressure Distributions for Bodies of Revolution at Transonic Speeds," NASA TN D-7331, 1973.
- ⁴¹Whitfield, J.D., Griffith, B.J., Bang, C., and Butler, R.W., "Overview of Flight and Ground Testing with Emphasis on the Wind Tunnel," AIAA Paper 81-2474, Nov. 1981.
- ⁴²Dougherty, N.S. Jr. and Fisher, D.F., "Boundary-Layer Transition on a 10-Deg Cone: Wind Tunnel/Flight Correlation," AIAA Paper 80-0154, Jan. 1980.
- ⁴³Webb, L.D., Whitmore, S.A., and Janssen, R.L., "Preliminary Flight and Wind Tunnel Comparisons of the Inlet/Airframe Interaction of the F-15 Airplane," AIAA Paper 79-0102, Jan. 1979.
- ⁴⁴Nugent, J., Taillon, N.V., and Pendergraft, O.C. Jr., "Status of a Nozzle-Airframe Study of a Highly Maneuverable Fighter," AIAA Paper 78-990, July 1978.
- ⁴⁵Plant, T.J., Nugent, J., and Davis, R.A., "Flight-Measured Effects of Boattail Angle and Mach Number on the Nozzle Afterbody Flow of a Twin-Jet Fighter," AIAA Paper 80-0110, Jan. 1980.
- ⁴⁶*YF-12 Experiments Symposium*, Vol. 3, NASA CP-2054, 1978.
- ⁴⁷"Preliminary Analysis of STS-1 Entry Flight Data," NASA TM-81363, 1981.